arXiv:2011.13193v1 [cond-mat.supr-con] 26 Nov 2020

Enhancement of maximum superconducting temperature by applying pressure and reducing the charge transfer gap

Yi-Hsuan Liu[1,2*] , Huan-Kuang Wu[3] and Ting-Kuo Lee[2,4]

[1] *Department of Physics, National Tsing Hua University, Hsinchu 30013, Taiwan*

[2] *Institute of Physics, Academia Sinica, Nankang 11529, Taiwan*

[3] *Department of Physics, University of Maryland, College Park, MD 20742, USA*

[4] *Department of Physics, National Sun Yat-sen University, Kaohsiung 80424, Taiwan*

[*] *yhliu0043@gapp.nthu.edu.tw*

Abstract

Recent Scanning Tunneling Spectra(STS) measurement on underdoped cuprate discovers the increase of the maximum superconducting transition temperature T_c when the size of charge transfer gap (CTG) is reduced. Applying pressure is another well known method to increase maximum T_c. However, these pressure experiments also found another puzzle that T_c is enhanced in underdoped and optimal doped samples but suppressed in overdoped. Here we present a possible mechanism based on the charge fluctuation to explain both these two effects simultaneously. Starting from 3-band Hubbard model, we retrieve the charge fluctuation(CF) between oxygen $2p^6$ band and copper $3d^{10}$ band which is ignored in the $t-J$ model. This model is studied via variational Monte Carlo method(VMC).

Keywords: cuprate, high-temperature superconductor, t-J model, t-J-U model, VMC

1. Introduction

About 30 years ago, right after the discovery of high temperature superconductor[1–5] (HTS), Anderson[6] has proposed that this system is a Mott insulator at half filling. Either the strong coupling one-band Hubbard model or its equivalent low-energy $t-J$ model is a good starting Hamiltonian to understand the physics. Later, it was shown by Emery [7] that the half-filled cuprate with both copper and oxygens considered is actually a charge transfer insulator to be described by a three-band Hubbard model. Not long after, Zhang and Rice[8, 9] showed that the large charge transfer gap could help to form a singlet state, known as Zhang-Rice singlet (ZRS), representing the doped hole. Therefore, the system could still be considered as an effective one-band model. In this case, the oxygen charge degrees of freedom are effectively frozen. Also, there are a number of experiments to support the presence of ZRS[10–12].

Many works tried to search for the dominant factors to enhance the superconducting transition temperature T_c, for example, the number of layers, the distance of apical oxygen, the magnetism, the hole density of Cu and O and the charge transfer gaps, etc. Few years ago, Weber et.al[13, 14] have shown that the maximum T_c or T_c^{max} becomes larger with the decreasing charge transfer energy, increasing nearest hopping $|t'|$ and apical oxygen distance. Recently several experiments have provided evidences to reexamine this idea of one-band model beyond optimal doping[15–17]. The charge transfer gap (CTG) was directly measured by using the scanning tunneling microscopy(STM) for one and two layers $Bi_2(Sr,La)_2CuO_{6+\delta}$(Bi-2201) and $Ca_2CuO_2Cl_2$(CCOC)[18]. Not only the gap size is surprisingly small of the order of $1-2$ eV, but the maximum superconducting temperature T_c^{max} is higher for the smaller gap. The result is also confirmed by angle-resolved photoemission spectroscopy (ARPES)[19]. Thus the magnitude of the CTG is about same order of magnitude as the hopping energy between oxygen p orbital and copper d orbital, clearly we need to have a re-examination of the CF effect.

The effect of charge transfer between Cu3d^{10} and O2p^6, which shall be denoted as CF hopping in this paper, is also examined by a number of other experiments. For example, applying hydrostatic [20, 21] and uniaxial pressure[22], will enhance T_c^{max}. However, a puzzling phenomena [23] is the reduction of T_c with pressure in the overdoped (OD) regime but enhancement of T_c in the underdoped (UD) and optimal doping regimes, it leads to the shift of the T_c dome to lower dopant density and with enhancement of T_c^{max}. This unusual behavior for T_c under pressure cannot be simply attributed to the change of lattice constant or carrier density. A theoretical understanding is still lacking. We will show below that proper consideration of CF hopping provides a simple explanation of enhancement of T_c^{max} and the oppostie behavior in the UD and OD regimes.

Before we start to present the details on our model and calculations, we note that the model without explicitly including oxygen has successfully explained a number of experiments. However, to study the CF effect, we will have to bring back the oxygen degrees of freedom. Instead of taking into account of the full degree of freedom of oxygen which will require extensive numerical works, in this paper we will present an effective model that keeps the ZRS but includes the CF effect to reveal the physics.

We will start with the Emery's 3-band mode [7]:

$$\hat{H}_U = \sum_{l,\sigma} \epsilon_p p^\dagger_{l,\sigma} p_{l,\sigma} + \sum_{i,\sigma} \epsilon_d d^\dagger_{i,\sigma} d_{i,\sigma} + \sum_{i,\sigma} U_d \hat{n}^d_{i\uparrow} \hat{n}^d_{i\downarrow} \tag{1}$$

$$\hat{H}_{pd} = -\sum_{i,\sigma} \sum_{l \subset i} t_{pd} V_{il} d^\dagger_{i,\sigma} p_{l,\sigma} + h.c \tag{2}$$

where l runs over the four oxygen around a copper, and $V_{il} = 1$ for $l = i + \frac{1}{2}x$ and $i + \frac{1}{2}y$, while $V_{il} = -1$ for $l = i - \frac{1}{2}x$ and $i - \frac{1}{2}y$. $d^\dagger_{i,\sigma}$ creates a d-hole with spin σ in the Cu($d_{x^2-y^2}$) at site i, $p^\dagger_{j,\sigma}$ creates a p-hole with spin σ in the O(p_x and p_y) orbitals at site j. ϵ_d and ϵ_p correspond to the energy of the local Cu($d_{x^2-y^2}$) and O(p_x and p_y) orbital, respectively. U_d is on-site Coulomb repulsion, of copper. The vacuum is defined as Cu d^{10} and O p^6.

At half-filling, i.e., before a hole or an electron is doped into the system, every Cu will be at d^9 state with a single hole and all oxygens are at p^6 without holes and the system is a Mott insulator and a spin-1/2 quantum Heisenberg system [6]. To consider the effect of doping, Zhang and Rice[8, 9] have derived an effective single-band model from Emery's 3-band model. In their argument , when a hole is doped into a cuprate, it will reside on oxygen. However, the superexchange coupling between this hole's spin and the spin at the nearest neighbor Cu d^9 site will form a ZRS spin singlet. All the other triplet and nonbonding state have much higher energies and could be neglected from the low energy Hamiltonian. In this picture, the hole's energy on oxygen site is actually the ZRS state with energy $\tilde{\epsilon}_p$, where the tilde means a renormalized energy of ϵ_p. If the only charge degrees of freedom considered is from the doped holes that forming ZRS, then the degrees of freedom left are the original spin -1/2 on the Cu d^9 site and doped holes or ZRSs and then we obtain the well-known $t-J$ Hamiltonian[9].

$$\hat{H}_{t-J} = -t \sum_{\langle i,j \rangle} P_G c^\dagger_i c_j P_G + J \sum_{\langle i,j \rangle} (\vec{S}_i \cdot \vec{S}_j - \frac{1}{4} n_i n_j) \tag{3}$$

where $P_G = \prod_i (1 - \hat{n}_{i\uparrow}\hat{n}_{i\downarrow})$, t is the effective hopping amplitude of ZRS, and J is the superexchnage interaction between nearest neighbor Cu d^9 holes.

However, in principle several other charge degrees of freedom could be important. One possibility is that instead of being at the oxygen, the hole could sit at the Cu site to form Cu d^8 which has energy $2\epsilon_d + U_d$ according to Eq. (1). This could be neglected at large U_d. The other possibility is to have the hole hopping from the Cu d^9 site to the nearest oxygen site to form a ZRS with the adjacent Cu while leaving a Cu d^{10} behind. This is schematically shown in Fig.1a. The energy difference between the initial and final configurations of this process is $\tilde{\epsilon}_p$ - ϵ_d, which is exactly the charge transfer gap, Δ_{CT}, discussed before. If only this process is to be considered besides t and J, we could completely eliminate the oxygen and denote the two configurations as in Fig.1b, where the Cu d^{10} is now represented by a doublon. The rate of this

process switching from a pair of nearest-neighbor holes to a holon-doublon pair is denoted as $\bar{t}$. Once we have Cu d^{10} as a doublon, then it can also exchange with a Cu d^9 through the middle oxygen as shown in Fig. 1c. This is equivalent to the hopping of a doublon, as shown in Fig.1d. Finally, we have an effective one-band charge transfer model

$$\hat{H}_{CT} = \hat{H}_{t-J} + \hat{H}_{CF} \tag{4}$$

$$\begin{aligned}\hat{H}_{CF} = &- \bar{t} \sum_{\langle i,j\rangle\sigma} (1-\hat{n}_{i,\bar{\sigma}})c^{\dagger}_{i\sigma}c_{j,\sigma}\hat{n}_{j,\bar{\sigma}} + \hat{n}_{i,\bar{\sigma}}c^{\dagger}_{i\sigma}c_{j,\sigma}(1-\hat{n}_{j,\bar{\sigma}}) + h.c \\ &- t_d \sum_{\langle i,j\rangle\sigma} \hat{n}_{i,\bar{\sigma}}c^{\dagger}_{i\sigma}c_{j,\sigma}\hat{n}_{j,\bar{\sigma}} + h.c \\ &+ \Delta_{CT}\sum_i \hat{n}_{i,\uparrow}\hat{n}_{i,\downarrow}\end{aligned} \tag{5}$$

where $\langle i,j\rangle$ denotes nearest neighboring sites. There are three kinds of nearest neighboring hoppings as shown schematically in Table.1. First, t is the hopping of ZRS or hole in the $t-J$ model. Second, $\bar{t}$ controls the creation and annihilation of a holon-doublon pair. Finally, t_d describes doublon hopping. We notice that the process of creation and annihilation of a holon-doublon pair is actually one of the many intermediates states considered in the derivation of the superexchange J[6, 8, 9]. Thus in principle J should be reduced from the values used in the pure $t-J$ model by a small amount. Thus in this work we consider a small $J/t = 0.33$. The generic parameter J ranges from 0.1 eV to 0.13 eV among various cuprates, which has been determined systematically by Raman scattering[24, 25] and neutron scattering[26, 27].

By setting $t = \bar{t} = t_d$, the model is equivalent to the $t-J-U$ model where Δ_{CT} is the effective Hubbard U. The model[28–33] has been studied via various method like variational Monte Carlo (VMC) method [34–37], slave-particle method[38, 39] , Gutzwiller renormalized mean field theory(RMFT) [40–46], diagrammatic expansion of the Gutzwiller wave function (DE-GWF)[47–49] , and density matrix renormalization group(DMRG)[28, 50]. To examine CF effect more carefully, we will consider more general cases where the three hopping amplitudes, t, $\bar{t}$ and t_d, are different. Their difference will become apparent when we discuss the effect of pressure in Sec.3.3. The derivation of these parameters from the 3-band model of Eqs. (1) and (2) are quite tedious[51]. They depend on CTG, hybridization t_{pd} and $d-d$ Coulomb repulsion U_d. In this work, we will just treat these as parameters of our model.

t	$\underline{\uparrow}\,\underline{0}$	$\Longleftrightarrow$	$0\,\underline{\uparrow}$
$\bar{t}$	$\underline{\uparrow}\,\underline{\downarrow}$	$\Longleftrightarrow$	$\underline{0}\,\underline{\uparrow\downarrow}$
t_d	$\underline{\uparrow\downarrow}\,\underline{\downarrow}$	$\Longleftrightarrow$	$\underline{\downarrow}\,\underline{\uparrow\downarrow}$

Table 1: Classification of hopping

This paper is organized as follows. In Section.2 the wave function used in the VMC method is presented. The effect of the three CF parameters: $\bar{t}$, t_d and Δ_{CT} are analyzed in Section.3.1. In Section. 3.2 we discuss the relation between CTG and pairing magnitude. In Section 3.3, we discuss the effect of pressure on pairing. Finally, the conclusion is given in Section. 4.

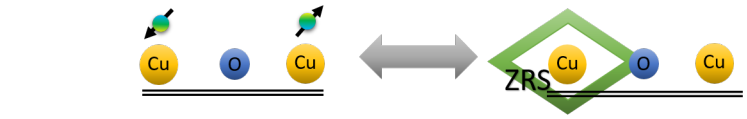
2. Formalism and Method

For the variational ground state ansatz in the VMC calculation, we use the correlated d-wave BCS wave function [52–56]

$$|\Psi\rangle = \hat{P}_G\hat{P}_{dh}\hat{P}_{N_e}|\Psi_{d-BCS}\rangle \tag{6}$$

where $\hat{P}_{Ne}$ is the projection operator to fix the total number of particles to be N_e and the d-wave BCS trial wave function[52, 53] is

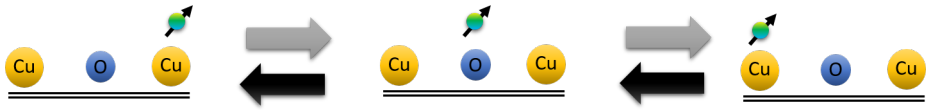
$$|\ \Psi_{d-BCS}\rangle = \prod_{k\subset BZ}(u_k + v_k c^{\dagger}_{k\uparrow}c^{\dagger}_{-k\downarrow})|0\rangle \tag{7}$$



(a) Three band picture of CF hopping.



(b) CF hopping in one band representation.



(c) Three band picture of doublon hopping.



(d) Doublon hopping in one band representation.

Figure 1: Mapping the CF hopping processes in three bands into our effective one-band model with schematic illustrations. (a)The initial state has an O2p^6 in between two neighboring Cu3d^9 holes with opposite spin. In the three-band model, one of these two holes on Cu site could hop to the middle O site to form a ZRS with the hole on the other Cu and leaving a Cu $3d^{10}$ or the doublon state. Hence this is equivalent to the formation of a holon-doublon pair in our one-band representation as shown in (b). (c) In the three-band model, the initial configuration of Cu3d^{10}, O2p^6 and Cu3d^9 could change to the intermediate configuration with Cu3d^{10}, O2p^5 and Cu3d^{10}, before it reaches the final configuration with Cu3d^9 O2p^6 and Cu3d^{10}, but this process is equivalent to the exchange between Cu $3d^{10}$ and neighboring Cu $3d^9$ which could be easily seen as the hopping of doublon in our representation shown in (d).

where $u_k = \frac{1}{2}(1 + \frac{\xi_k}{\sqrt{\xi_k^2+\Delta_k^2}})$, $u_k^2 + v_k^2 = 1$,$\xi_k = -2(cosk_x + cosk_y) - 4t_v' cosk_x cosk_y - \mu_v$, $\Delta_k = \Delta_v(cosk_x - cosk_y)$, t_v', μ_v and Δ_v are variaitonal parameters. $\hat{P}_G$ is the well-known Gutzwiller projector [57]

$$\hat{P}_G = \prod_i (1 - (1-g)\hat{n}_{i\uparrow} n_{i\downarrow}) \tag{8}$$

which controls the doublon density. For $g = 0$, there is no doublon and we have the strongest correlation in the large Δ_{CT} limit and this is used for the pure $t - J$ model. On the contrary, there is no correlation for $g = 1$. The Jastrow-type factor [58] $\hat{P}_{dh}$ is introduced to provide an attractive interaction between doublon and hole[59–61] to make sure at half-filling we recover the Mott insulator without free carrier, it is of the form

$$\hat{P}_{dh} = \prod_i (1 - Q_{dh}\hat{B}_i) \tag{9}$$

where $\hat{B}_i = \prod_\tau \hat{d}_i(1 - \hat{h}_{i+\tau}), \tau = \hat{x}, \hat{y}$ represents a nearest neighbor holon-doublon binding state, $\hat{d}_i$ is the doublon creation operator $\hat{d}_i = c_{i\uparrow}^\dagger c_{i\uparrow} c_{i\downarrow}^\dagger c_{i\downarrow}$ and $\hat{h}_i$ is the hole creation operator $\hat{h}_i = (1 - c_{i\uparrow}^\dagger c_{i\uparrow})(1 - c_{i\downarrow}^\dagger c_{i\downarrow})$. For $Q_{dh} = 0$, doublon and hole are free, while for $Q_{dh} = 1$ doublon cannot be separated from a hole. For $Q_{dh} < 0$ doublon and hole are repulsive to each other. In our case, for large Δ_{CT}, Q_{dh} is always positive.

In order to find the ground state we optimize the trial wavefunction by implementing the stochastic reconfiguration(SR) method described in detail in Ref.[62]

The superconductivity is characterized by the d-wave pairing order parameter

$$\Delta_{SC} = \sum_i < c_{i\uparrow} c_{i+x\downarrow} > -(x \leftrightarrow y)$$

However, in canonical VMC, what we can measure is the pair-pair correlation function

$$P(\vec{r}) = \frac{1}{N_s}\sum_i \Delta^\dagger(\vec{R}_i)\Delta(\vec{R}_i + \vec{r})$$

where N_s is the number of the sites and

$$\Delta(\vec{R}_i) = \frac{1}{\sqrt{2}}(\langle c_{i\uparrow}c_{i+x\downarrow} - c_{i\downarrow}c_{i+x\uparrow}\rangle - (x \leftrightarrow y))$$

By taking the square root of the pair-pair correlation at the maximum distance, r_{max}, we can estimate the magnitude of pairing order parameter.

$$\Delta_{SC} \simeq \sqrt{P(\vec{r}_{max})}$$

3. Results

As mentioned above, the three hopping amplitudes in Table.1 are not necessarily the same. In this section, we investigate the effect of varying $\bar{t}$, t_d and Δ_{CT} with fixed $t = 1$ and $J = 0.33$. Throughout this work, the lattice size considered is 20×20. In the main text we will show the result of having only the nearest neighboring hopping terms. A very similar result is obtained by including the second nearest neighboring hopping terms where we set $t'/t = \bar{t}'/\bar{t} = t'_d/t_d = -0.3$ which is presented in the Supplementary Material.

3.1. Tuning parameters $\bar{t}$, t_d and Δ_{CT}

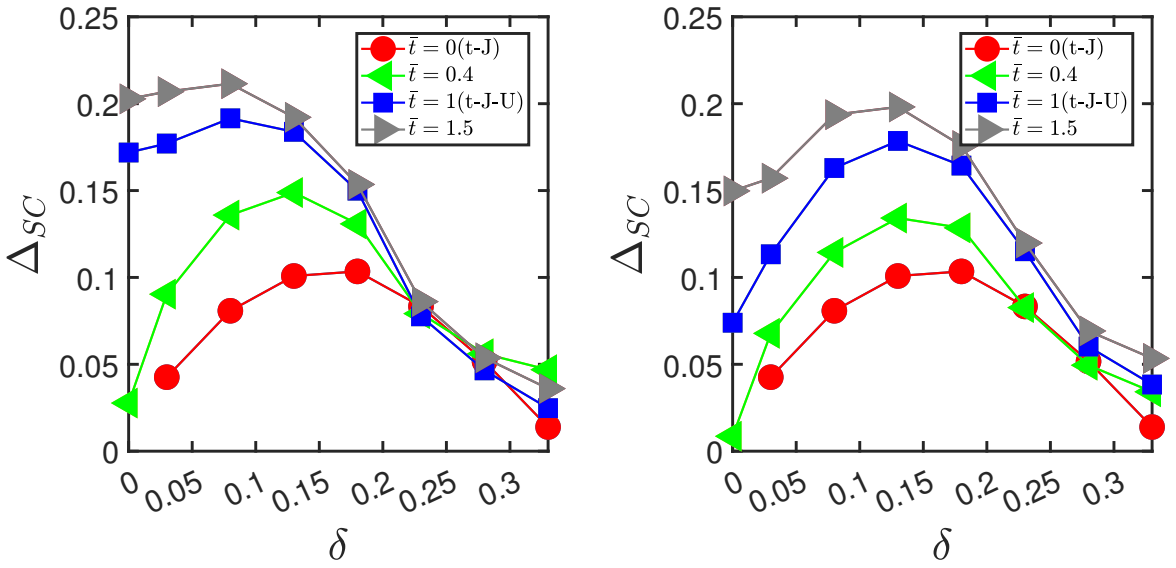
In this section, we show the d-wave pairing order parameter as a function of dopant concentration with varying $\bar{t}$, t_d or Δ_{CT} in Figs. 2, 3 and 4 respectively.

First, we consider two cases with $\Delta_{CT} = 6$ and $\Delta_{CT} = 8$ in Figs 2a and 2b, respectively. By fixing $t_d = 1$, the CF process is only related to the formation of holon-doublon pair as shown in Fig. 1b. Three hopping amplitudes $\bar{t} = 0.4$, 1 and 1.5 has been shown in the figure. Note that the label $\bar{t} = 0$ corresponds to the $t-J$ model, while for $\bar{t} = 1$, it becomes the $t-J-U$ model. Clearly, pairing is enhanced strongly in the underdoped(UD) regime as $\bar{t}$ increases. This enhancement of pairing can be understood by the increase in the effective superexchange interaction arises from the additional $\bar{t}$ process. When there is a larger Δ_{CT} and a smaller $\bar{t}$, the CF is less important and the result is closer to that of the $t-J$ model. Thus CT is effectively reducing the Hubbard U. We also note that when $\bar{t}$ gets larger there is apparent finite superconductivity at very low doping, which is known as the Gossamer superconductivity[30, 31, 40].

In Fig. 3, we study the effect of t_d. The d-wave pairing order parameter as a function of dopant concentration for $t_d = 0$, 0.5, 1 and 1.3 is shown in Fig. 3a and 3b for $\Delta_{CT} = 6$ and $\Delta_{CT} = 8$, respectively. Notice here we set that $\bar{t} = 1$. By increasing t_d, we found pairing at UD regime is slightly enhanced but suppressed at the OD. Similar to the effect of $\bar{t}$, increasing t_d enhances CF and suppresses strong correlation. The suppression of pairing in the OD regime is due to the lack of singly occupied spin-1/2 particles or spinons, which effectively reduces the number of electrons available for pairing. The controlling parameter of spinon density and how it affects pairing will be elaborated further in the next section.

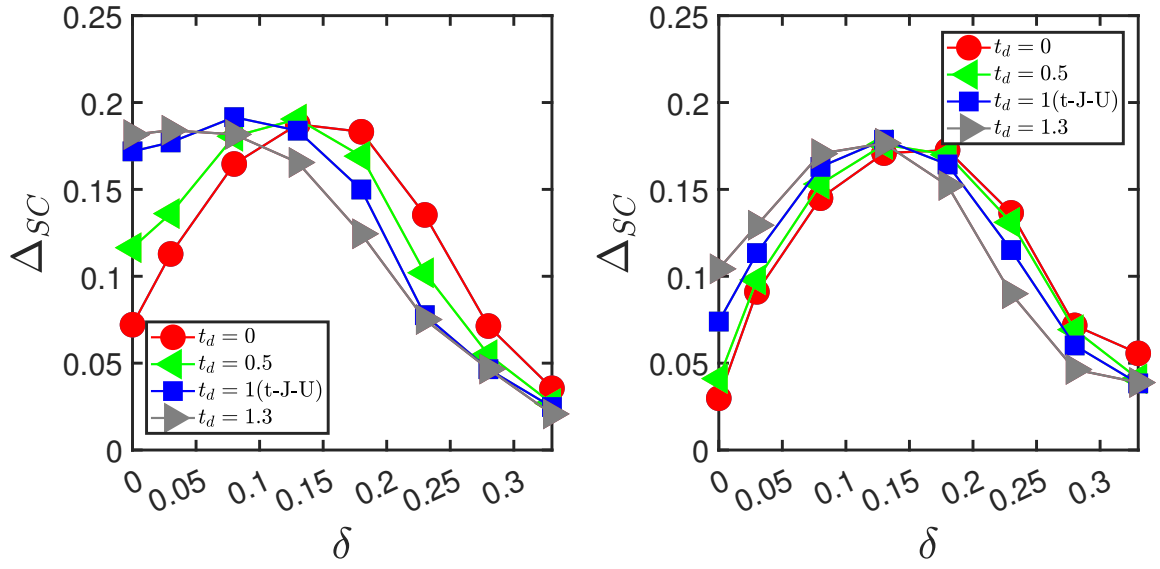
In Fig 4, we show the d-wave pairing order parameter as a function of dopant concentration for $t_d = 1$ and three different CTG, $\Delta_{CT} = 6$, 8 and 10. Fig. 4a is for $\bar{t} = 1$ and 4b for 1.5. Similar to the result of large t_d or $\bar{t}$, smaller Δ_{CT} enhances pairing in the UD regime but suppress it in the OD side.

All the results shown in Figs. 2-4 reveal a consistent physical picture. When Δ_{CT} becomes smaller or $\bar{t}$ or t_d becomes larger, maximum SC order parameter increases and the pairing dome moves toward the smaller dopant concentration. In addition we found qualitatively similar result with the $t-J-U$ model for various values of $\bar{t}$ and t_d. On the other hand, the "shift" of pairing dome in Fig. 4 is very similar to the high pressure experiment result on Hg1212 [23]. This will be discussed further in Sec.3.3



(a) (b)

Figure 2: Pairing order parameter as a function of dopant concentration for various $\bar{t}$. Here we have $t_d = 1$. The CTG is set to (a)$\Delta_{CT} = 6$ and (b)$\Delta_{CT} = 8$. Note that the label $\bar{t} = 0$ stands for $\bar{t} = t_d = 0$ which is the same as the $t - J$ model. For the case $\bar{t} = 1$, we have the $t - J - U$ model.



(a) (b)

Figure 3: Pairing order parameter correlation as a function of dopant. The CTG is set to (a)$\Delta_{CT} = 6$ and (b)$\Delta_{CT} = 8$. The hopping parameter is $t = \bar{t} = 1$ $J = 0.33$.

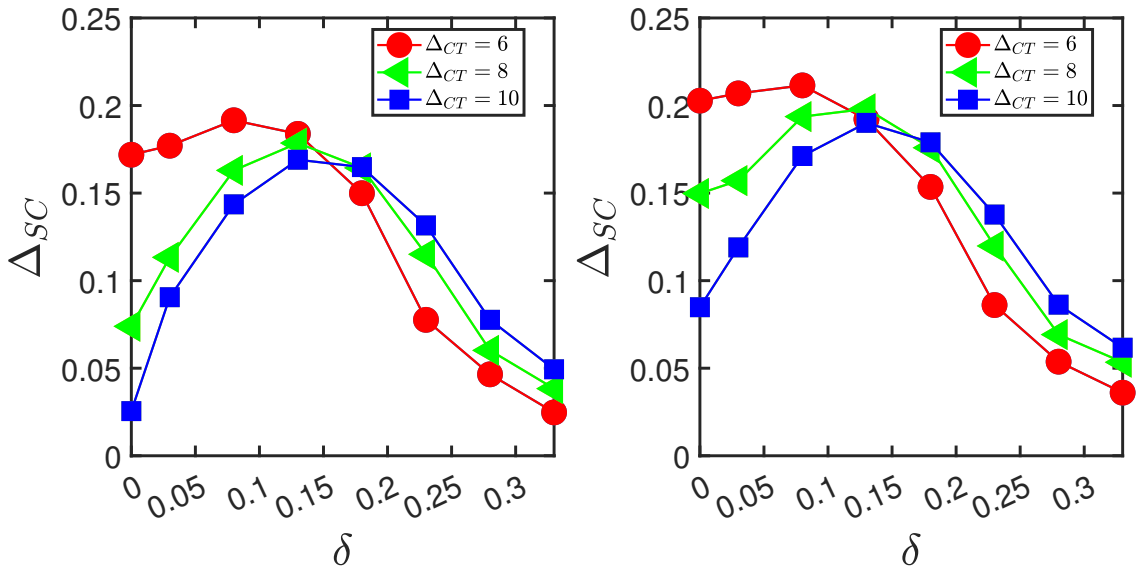


Figure 4: Pairing order parameter as a function of dopant density with three different values of CTG. The hopping parameter is $t_d = 1$ and (a) is for $\bar{t} = 1$ and (b) is for $\bar{t} = 1.5$.

3.2. Relation of CTG and pairing amplitude

Recently, Ruan *etal*. [18] found anti-correlation between T_c^{Max} and CTG in both single- and double-layered cuprate via scanning tunneling spectroscopy(STS). To investigate the anti-correlation, we determine the maximum pairing amplitude, Δ_{SC}^{Max}, as a function of the CTG by calculating the paring amplitude as a function of hole density. In Fig. 5, for small Δ_{CT} or effective U, where Gossamer superconductivity[30, 31, 40] dominates, Δ_{SC}^{Max} is approximately proportional to Δ_{CT} with almost the same slope. This can be explained simply. As Δ_{CT} increases from 0, doublon number begins to decrease significantly and consequently the number of singly occupied sites or spinon increases (see Fig. 6a). Once the CTG values reach a critical magnitude, the strong correlation Mott physics begins to take hold, then the increase of Δ_{CT} will result in a decrease of pairing order which should be inversely proportional to the CTG in the form of t^2/Δ_{CT}. This is consistent with the result in Ref. [18] that T_c^{max} is roughly proportional to $1/\Delta_{CT}$ for one- and two-layer cuprates. Their data also shows when the CTG is reduced by 25% from one layer CCOC to Bi2201, the T_c^{max} increases 45%. By choosing $t = 0.3eV$ and consider $\bar{t} = 0.4t$, we get the enhancement of maximum pairing amplitude about 23% when Δ_{CT}/t is reduced from 6.5 to 5. This result is quite satisfactory considering that the parameters of these two different cuprates are roughly estimated.

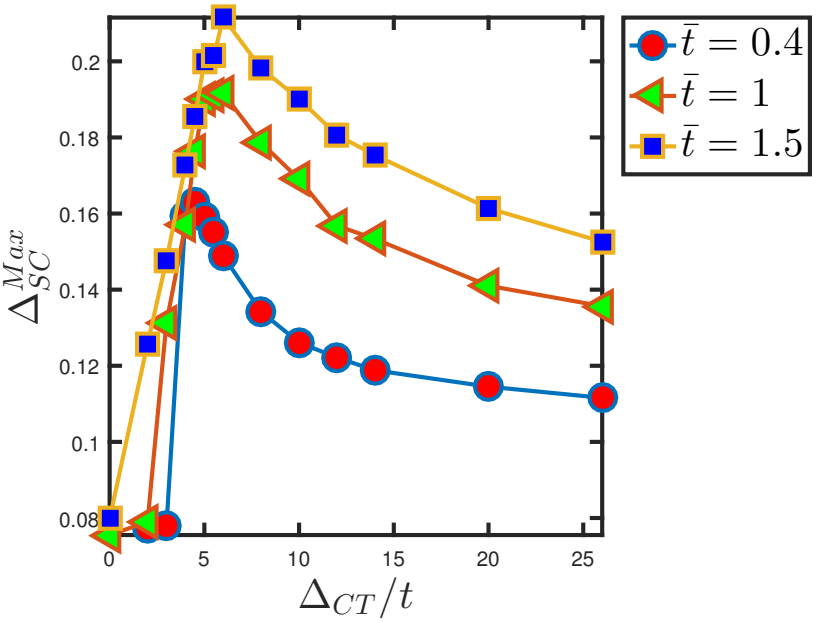


Figure 5: Maximum d-wave pairing order parameter vs. CTG with $t_d = 1$ and $t' = 0$.

Since the introduction of the CTG provides an additional superexchange interaction for pairing, this sure will enhance Δ_{SC}^{Max} and T_c^{Max}. However, we were surprised to find that pairing order parameter is not uniformly enhanced for all the doped hole density when CTG is reduced as shown in Fig. 4. The enhancement is larger in the UD regime and with no enhancement or pairing is even suppressed in the OD phase. As noted by Anderson[6] a long time ago, the d-wave pairing caused by the superexchange interaction favors the singly occupied sites or spinons. In Fig 6a, we examine the effect of spinon density on pairing. The parameters used are $\bar{t} = t_d = t$, $J = 0.33$ and $t' = t'_d = \bar{t}' = 0$ so this is same as $t - J - U$ model. For all the concentrations, the spinon density first increases quickly with CTG and then approaches a plateau with a very small increase around $\Delta_{CT} = 8 - 10$ which enters the strong correlation regime. The increase of spinon density is much rapid and larger in the UD regime than in OD regime. Thus we can expect pairing will be quickly enhanced in the UD regime but much milder in the OD regime. Accordingly, one would also expect Δ_{SC}^{Max} to be larger in the UD regime. This is exactly what we found in Fig. 6b, where the pairing order parameter is plotted as a function of CTG for various hole densities. For hole density less than 0.18, the pairing order rapidly increases with CTG. Once the maximum value is reached at some critical CTG, the system enters the strongly correlated regime and the increase of Δ_{CT} only reduces the additional superexchange interaction thus pairing order decreases as $1/\Delta_{CT}$. At very large values of Δ_{CT}, the system is essentially the same as the $t - J$ model and the pairing order is quite small as it is proportional to the hole density in the UD regime. In the OD regime, although the spinon density still gradually increases as CTG is increased, it is weaker than the effect of decreases of additional superexchange interaction as $1/\Delta_{CT}$.

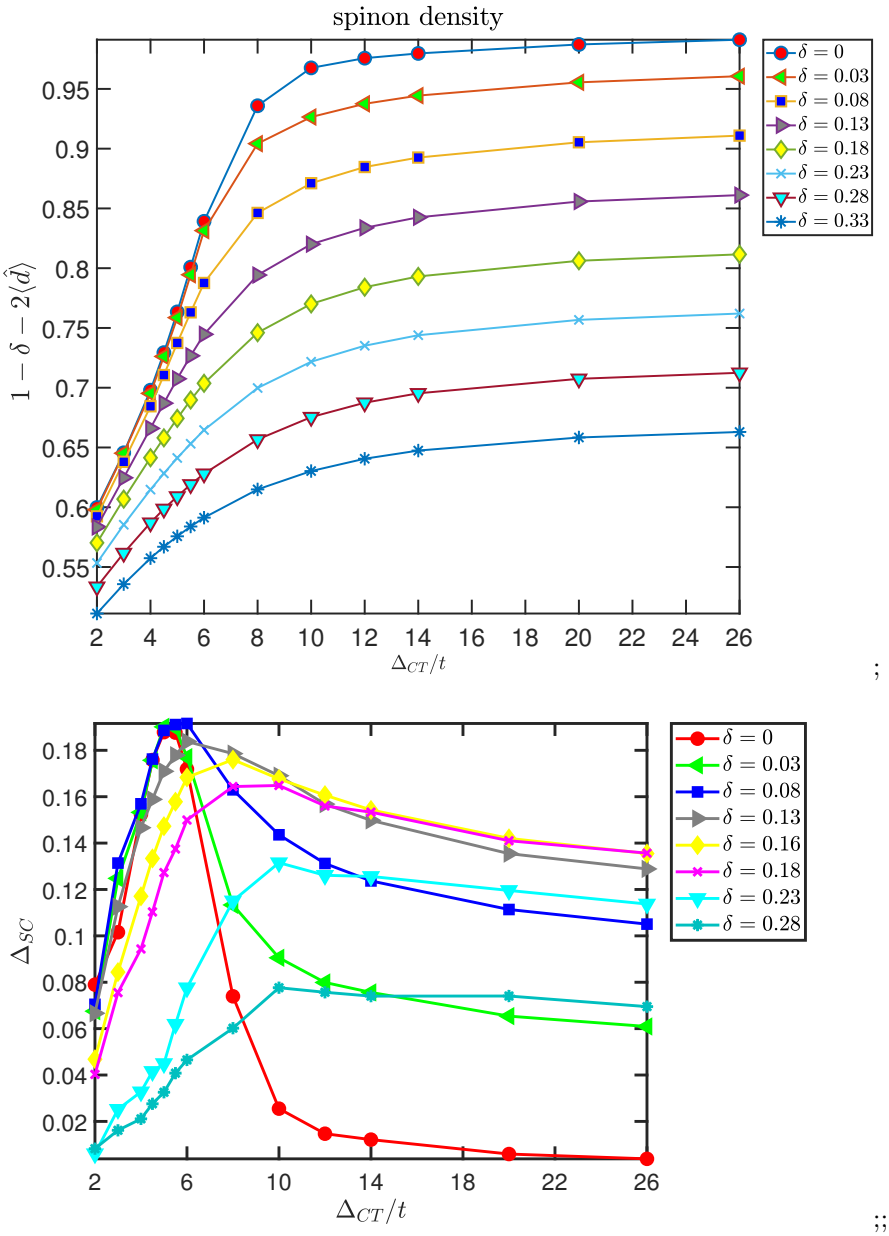


Figure 6: (a)spinon density as a function of Δ_{CT}. (b)Pairing order parameter as a function of Δ_{CT}. The parameters are $\bar{t} = t_d = 1$ and $t' = 0$.

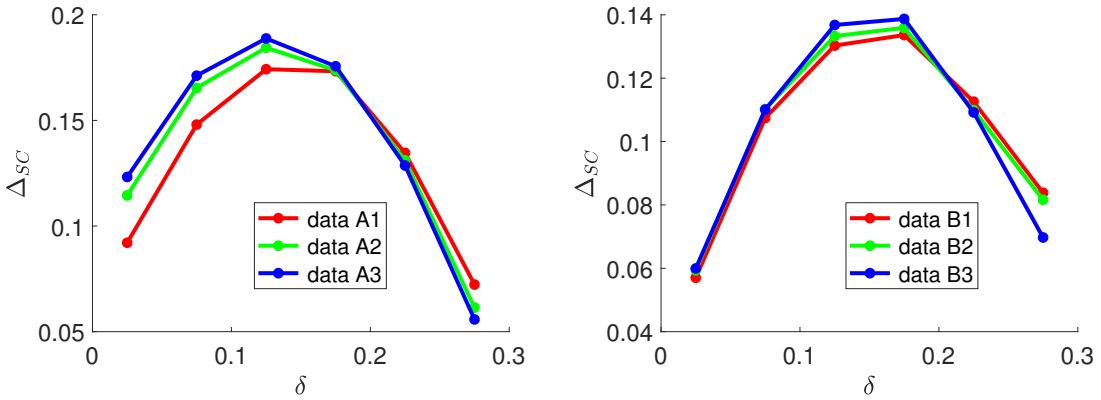
3.3. Examine the effect of pressure

When pressure is applied, the in-plane distance between Cu and Oxygen will decrease, hence t_{pd} will increase. As shown from previous sections, not only Δ_{CT} but also t_d and $\bar{t}$ can affect the superconducting dome shape. According to standard perturbation derivation: $t \sim t_{pd}^2$, $\bar{t} \sim t_{pd}$, $t_d \sim t_{pd}^2$, $J \sim t_{pd}^4$. Hence as t_{pd} increases, t_d/t hardly changes, $\bar{t}/t$ is inversely proportional to t_{pd}, thus it will decreases, Δ_{CT}/t will decreases as $1/t_{pd}^2$. and J/t is proportional to t_{pd}^2. So assuming that we set the parameter at ambient pressure(J/t, Δ_{CT}/t, t_d/t, $\bar{t}/t$) to be (0.33, 8, 1, 1). If we increase t_{pd} by a ratio α then the parameters will turn into $(0.33\alpha^2, 8/\alpha^2, 1, 1/\alpha)$. As pressure is increased, α increases from 1 to 1.04 and 1.08 as shown in Table 2 with all other parameters. In Fig.7, the two sets of parameters show the similar result that as

pressure or t_{pd} increases, pairing order parameter increases in UD regime but decreases in OD. This is very consistent with high pressure experiment[23].

Table 2

data label	A1	A2	A3	B1	B2	B3
α	1	1.04	1.08	1	1.04	1.08
J/t	0.33	0.357	0.385	0.33	0.357	0.385
Δ_{CT}/t	8	7.4	6.86	8	7.4	6.86
t_d/t	1	1	1	0.5	0.5	0.5
$\bar{t}/t$	1	0.961	0.926	0.4	0.384	0.37



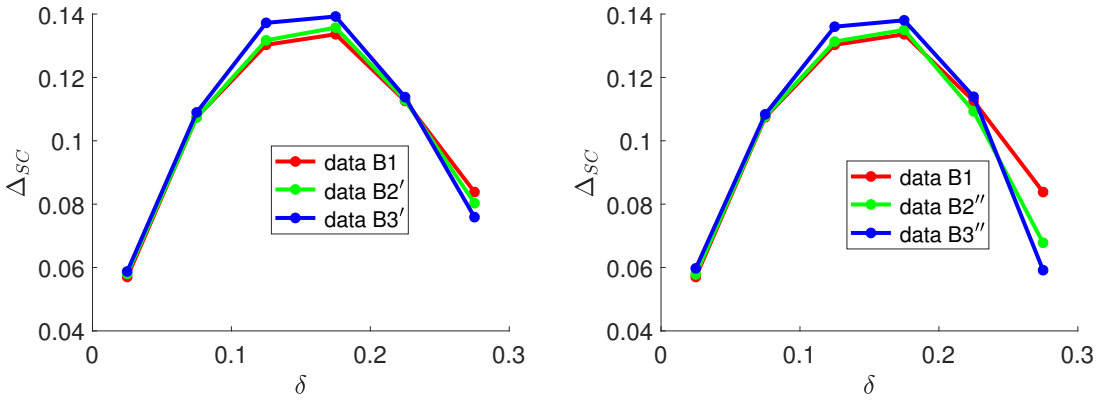
(a) (b)

Figure 7: Simulation of pressure effect, parameter at ambient pressure(J/t, Δ_{CT}/t, t_d/t, $\bar{t}/t$) are seleted to be (0.33, 8, 1, 1) for (a) and (0.33, 8, 0.5, 0.4) for (b). The detail parameters are listed in Table.2

On the other hand, the hydrostatic pressure will also decrease the apical oxygen distance. When the apical Oxygen is brought closer to the Cu atom, it will increase the repulsion to electrons on the copper, hence the increase of charge transfer gap[63, 64]. distance. To simulate this effect, we increase Δ_{CT} a little bit, say 2.5% or 5%. Assuming at ambient pressure the parameter (J/t, Δ_{CT}/t, t_d/t, $\bar{t}/t$) is (0.33, 8, 0.5, 0.4) as data of B1 in Table 2, With increasing pressure, the t_{pd} becomes αt_{pd} and Δ_{CT} becomes $\beta\Delta_{CT}$. Hence, as pressure is applied, the parameters becomes ($0.33\alpha^2$, $8\beta/\alpha^2$, 0.5, $0.4/\alpha$). The detailed parameters are listed in Table.3. Fig. 8 shows similar result as Fig. 7 although we have included the effect that CTG is increased by reducing the apical oxygen distance from Cu. The UD side has its pairing enhanced while the OD side is reduced under pressure as the pairing dome is shifted or tilted toward the UD side.

Table 3

data label	B1	$B2'$	$B3'$	$B2''$	$B3''$
α	1	1.04	1.08	1.04	1.08
β	1	1.025	1.025	1.05	1.05
J/t	0.33	0.357	0.385	0.357	0.385
Δ_{CT}/t	8	7.58	7.03	7.77	7.2
t_d/t	0.5	0.5	0.5	0.5	0.5
$\bar{t}/t$	0.4	0.384	0.37	0.384	0.37



(a) (b)

Figure 8: Simulation of pressure effect that include the apical oxygen effect, parameter at ambient pressure(J/t, Δ_{CT}/t, t_d/t, $\bar{t}_/t$) are seleted to be (0.33, 8, 0.5, 0.4). As pressure is applied, the parameters becomes (0.33α, $8\beta/\alpha^2$, 0.5, $0.4/\alpha$)The detail parameter for the data is listed in Table.3

4. Conclusion

In summary, motivated by the recent experiments [65], we have studied the CF effect of the Copper-Oxygen three-band model with an effective one-band model similar to the t-J-U model. But now U or Δ_{CT} is the charge transfer gap. The formation of this doublon and its hopping as well as the size of the charge transfer gap all played an important role in the CF effect. The inclusion of these effects provides a simple understanding of the enhancement of maximum pairing when the Δ_{CT} is reduced as observed by the experiment [18]. Additionally, we also found that there is a minimum Δ_{CT} for enhancement. On the other hand, this enhancement only occurs in the UD regime but not in OD. This dichotomy between UD and OD is further examined by considering the effect of applying pressure. Our model provides a very simple explanation for the observations in several pressure experiments that T_c is always enhanced in the UD regime but reduced in the OD.

Acknowledgement

YHL and TKL were supported by Taiwan Ministry of Science and Technology Grant 108-2112-M-110-015. The calculation was supported by Academia Sinica Grid-computing Center(ASGC) and National Center for High Performance Computing in Taiwan.

References

[1] J. G. Bednorz, K. A. Müller, Possible highTc superconductivity in the $Ba-La-Cu-O$ system, Zeitschrift für Physik B Condensed Matter 64 (2) (1986) 189. doi:10.1007/BF01303701.
URL http://dx.doi.org/10.1007/BF01303701

[2] M. K. Wu, J. R. Ashburn, C. J. Torng, P. H. Hor, R. L. Meng, L. Gao, Z. J. Huang, Y. Q. Wang, C. W. Chu, Superconductivity at 93 K in a new mixed-phase Y-Ba-Cu-O compound system at ambient pressure, Phys. Rev. Lett. 58 (1987) 908. doi:10.1103/PhysRevLett.58.908.
URL https://link.aps.org/doi/10.1103/PhysRevLett.58.908

[3] P. A. Lee, N. Nagaosa, X.-G. Wen, Doping a mott insulator: Physics of high-temperature superconductivity, Rev. Mod. Phys. 78 (2006) 17–85. doi:10.1103/RevModPhys.78.17.
URL https://link.aps.org/doi/10.1103/RevModPhys.78.17

[4] B. Edegger, V. N. Muthukumar, C. Gros, Gutzwiller–RVB theory of high-temperature superconductivity: Results from renormalized mean-field theory and variational Monte Carlo calculations, Advances in Physics 56 (6) (2007) 927–1033. doi:10.1080/00018730701627707.
URL https://doi.org/10.1080/00018730701627707

[5] M. Ogata, H. Fukuyama, The t – J model for the oxide high- T c superconductors, Reports on Progress in Physics 71 (3) (2008) 36501. arXiv:arXiv:1008.0522v1, doi:10.1088/0034-4885/71/3/036501.
URL http://stacks.iop.org/0034-4885/71/i=3/a=036501{%}5Cnpapers3://publication/doi/10.1088/0034-4885/71/3/036501

[6] P. W. ANDERSON, The Resonating Valence Bond State in La_2CuO_4 and Superconductivity, Science 235 (4793) (1987) 1196. arXiv:http://science.sciencemag.org/content/235/4793/1196.full.pdf, doi:10.1126/science.235.4793.1196.
URL http://science.sciencemag.org/content/235/4793/1196

[7] V. J. Emery, Theory of high-T_c superconductivity in oxides, Phys. Rev. Lett. 58 (1987) 2794. doi:10.1103/PhysRevLett.58.2794.
URL http://link.aps.org/doi/10.1103/PhysRevLett.58.2794

[8] F. C. Zhang, T. M. Rice, Effective Hamiltonian for the superconducting Cu oxides, Phys. Rev. B 37 (1988) 3759. doi:10.1103/PhysRevB.37.3759.
URL http://link.aps.org/doi/10.1103/PhysRevB.37.3759

[9] F. C. Zhang, T. M. Rice, Validity of the t - J model, Phys. Rev. B 41 (1990) 7243. doi:10.1103/PhysRevB.41.7243.
URL http://link.aps.org/doi/10.1103/PhysRevB.41.7243

[10] Y.-J. Chen, M. G. Jiang, C. W. Luo, J.-Y. Lin, K. H. Wu, J. M. Lee, J. M. Chen, Y. K. Kuo, J. Y. Juang, C.-Y. Mou, Doping evolution of Zhang-Rice singlet spectral weight: A comprehensive examination by x-ray absorption spectroscopy, Phys. Rev. B 88 (2013) 134525. doi:10.1103/PhysRevB.88.134525.
URL https://link.aps.org/doi/10.1103/PhysRevB.88.134525

[11] N. B. Brookes, G. Ghiringhelli, A.-M. Charvet, A. Fujimori, T. Kakeshita, H. Eisaki, S. Uchida, T. Mizokawa, Stability of the Zhang-Rice Singlet with Doping in Lanthanum Strontium Copper Oxide Across the Superconducting Dome and Above, Phys. Rev. Lett. 115 (2015) 027002. doi:10.1103/PhysRevLett.115.027002.
URL https://link.aps.org/doi/10.1103/PhysRevLett.115.027002

[12] M. Taguchi, A. Chainani, K. Horiba, Y. Takata, M. Yabashi, K. Tamasaku, Y. Nishino, D. Miwa, T. Ishikawa, T. Takeuchi, K. Yamamoto, M. Matsunami, S. Shin, T. Yokoya, E. Ikenaga, K. Kobayashi, T. Mochiku, K. Hirata, J. Hori, K. Ishii, F. Nakamura, T. Suzuki, Evidence for Suppressed Screening on the Surface of High Temperature $La_{2-x}Sr_xCuO_4$ and $Nd_{2-x}Ce_xCuO_4$ Superconductors, Phys. Rev. Lett. 95 (2005) 177002. doi:10.1103/PhysRevLett.95.177002.
URL https://link.aps.org/doi/10.1103/PhysRevLett.95.177002

[13] C. Weber, C. Yee, K. Haule, G. Kotliar, Scaling of the transition temperature of hole-doped cuprate superconductors with the charge-transfer energy, EPL (Europhysics Letters) 100 (3) (2012) 37001. arXiv:1108.3028, doi:10.1209/0295-5075/100/37001.
URL http://stacks.iop.org/0295-5075/100/i=3/a=37001?key=crossref.86f7be16c6aa6e8b19bb54661aca90d9

[14] C. Weber, What controls the critical temperature of high temperature copper oxide superconductors: insights from scanneling tunnelling microscopy, Science Bulletin 62 (2) (2017) 102. doi:https://doi.org/10.1016/j.scib.2016.12.007.
URL http://www.sciencedirect.com/science/article/pii/S2095927316305916

[15] S. Badoux, W. Tabis, F. Laliberté, G. Grissonnanche, B. Vignolle, D. Vignolles, J. Béard, D. A. Bonn, W. N. Hardy, R. Liang, N. Doiron-Leyraud, L. Taillefer, C. Proust, Change of carrier density at the pseudogap critical point of a cuprate superconductor, Nature 531 (7593) (2015) 210. arXiv:1511.08162, doi:10.1038/nature16983.
URL http://arxiv.org/abs/1511.08162

[16] C. Collignon, S. Badoux, S. A. A. Afshar, B. Michon, F. Laliberté, O. Cyr-Choinière, J.-S. Zhou, S. Licciardello, S. Wiedmann, N. Doiron-Leyraud, L. Taillefer, Fermi-surface transformation across the pseudogap critical point of the cuprate superconductor $La_{1.6-x}Nd_{0.4}Sr_xCuO_4$, Phys. Rev. B 95 (2017) 224517. doi:10.1103/PhysRevB.95.224517.
URL https://link.aps.org/doi/10.1103/PhysRevB.95.224517

[17] N. Doiron-Leyraud, O. Cyr-Choinière, S. Badoux, A. Ataei, C. Collignon, A. Gourgout, S. Dufour-Beauséjour, F. F. Tafti, F. Laliberté, M.-E. Boulanger, M. Matusiak, D. Graf, M. Kim, J.-S. Zhou, N. Momono, T. Kurosawa, H. Takagi, L. Taillefer, Pseudogap phase of cuprate superconductors confined by Fermi surface topology, Nature Communications 8 (1) (2017) 2044. arXiv:1712.05113, doi:10.1038/s41467-017-02122-x.
URL http://www.nature.com/articles/s41467-017-02122-x

[18] W. Ruan, C. Hu, J. Zhao, P. Cai, Y. Peng, C. Ye, R. Yu, X. Li, Z. Hao, C. Jin, X. Zhou, Z.-Y. Weng, Y. Wang, Relationship between the parent charge transfer gap and maximum transition temperature in cuprates, Science Bulletin 61 (23) (2016) 1826. doi:10.1007/s11434-016-1204-x.
URL http://dx.doi.org/10.1007/s11434-016-1204-x

[19] S.-L. Yang, J. A. Sobota, Y. He, Y. Wang, D. Leuenberger, H. Soifer, M. Hashimoto, D. H. Lu, H. Eisaki, B. Moritz, T. P. Devereaux, P. S. Kirchmann, Z.-X. Shen, Revealing the Coulomb interaction strength in a cuprate superconductor, Phys. Rev. B 96 (2017) 245112. doi:10.1103/PhysRevB.96.245112.
URL https://link.aps.org/doi/10.1103/PhysRevB.96.245112

[20] Y. Cao, Q. Xiong, Y. Y. Xue, C. W. Chu, Pressure effect on the T_c of $HgBa_2CuO_{4+\delta}$ with $0.07 \leq \delta \leq 0.39$, Phys. Rev. B 52 (1995) 6854. doi:10.1103/PhysRevB.52.6854.
URL https://link.aps.org/doi/10.1103/PhysRevB.52.6854

[21] C. W. Chu, Y. Cao, Q. Xiong, Y. Y. Xue, δ-Influence on the pressure-effect on Tc of $HgBa_2CuO_{4+\delta}$ and the inverse parabolic Tc-relation, Journal of Superconductivity 8 (4) (1995) 393. doi:10.1007/BF00722813.
URL http://dx.doi.org/10.1007/BF00722813

[22] F. Hardy, N. J. Hillier, C. Meingast, D. Colson, Y. Li, N. Barišić, G. Yu, X. Zhao, M. Greven, J. S. Schilling, Enhancement of the Critical Temperature of $HgBa_2CuO_{4+\delta}$ by Applying Uniaxial and Hydrostatic Pressure: Implications for a Universal Trend in Cuprate Superconductors, Phys. Rev. Lett. 105 (2010) 167002. doi:10.1103/PhysRevLett.105.167002.

URL http://link.aps.org/doi/10.1103/PhysRevLett.105.167002
[23] A. Yamamoto, N. Takeshita, C. Terakura, Y. Tokura, High pressure effects revisited for the cuprate superconductor family with highest critical temperature, Nature Communications 6 (2015) 8990. doi:10.1038/ncomms9990.
URL http://www.nature.com/ncomms/2015/151201/ncomms9990/full/ncomms9990.html{#}ref4{%}5Cnhttp://www.nature.com/doifinder/10.1038/ncomms9990
[24] K. B. Lyons, P. A. Fleury, L. F. Schneemeyer, J. V. Waszczak, Spin fluctuations and superconductivity in $Ba_2YCu_3O_{6+\delta}$, Phys. Rev. Lett. 60 (1988) 732. doi:10.1103/PhysRevLett.60.732.
URL https://link.aps.org/doi/10.1103/PhysRevLett.60.732
[25] G. Blumberg, P. Abbamonte, M. V. Klein, W. C. Lee, D. M. Ginsberg, L. L. Miller, A. Zibold, Resonant two-magnon raman scattering in cuprate antiferromagnetic insulators, Phys. Rev. B 53 (1996) R11930. doi:10.1103/PhysRevB.53.R11930.
URL https://link.aps.org/doi/10.1103/PhysRevB.53.R11930
[26] P. Bourges, H. Casalta, A. S. Ivanov, D. Petitgrand, Superexchange coupling and spin susceptibility spectral weight in undoped monolayer cuprates, Phys. Rev. Lett. 79 (1997) 4906. doi:10.1103/PhysRevLett.79.4906.
URL https://link.aps.org/doi/10.1103/PhysRevLett.79.4906
[27] S. M. Hayden, G. Aeppli, R. Osborn, A. D. Taylor, T. G. Perring, S.-W. Cheong, Z. Fisk, High-energy spin waves in La_2CuO_4, Phys. Rev. Lett. 67 (1991) 3622. doi:10.1103/PhysRevLett.67.3622.
URL https://link.aps.org/doi/10.1103/PhysRevLett.67.3622
[28] S. Daul, D. J. Scalapino, S. R. White, Pairing correlations on $t-U-J$ ladders, Phys. Rev. Lett. 84 (2000) 4188. doi:10.1103/PhysRevLett.84.4188.
URL http://link.aps.org/doi/10.1103/PhysRevLett.84.4188
[29] S. Basu, R. J. Gooding, P. W. Leung, Enhanced bound-state formation in two dimensions via stripelike hopping anisotropies, Phys. Rev. B 63 (2001) 100506. doi:10.1103/PhysRevB.63.100506.
URL https://link.aps.org/doi/10.1103/PhysRevB.63.100506
[30] R. B. Laughlin, Gossamer superconductivity, arXiv:0209269 (2002).
[31] F. C. Zhang, Gossamer Superconductor, Mott Insulator, and Resonating Valence Bond State in Correlated Electron Systems, Phys. Rev. Lett. 90 (2003) 207002. doi:10.1103/PhysRevLett.90.207002.
URL http://link.aps.org/doi/10.1103/PhysRevLett.90.207002
[32] P. Coleman, Superconductivity: lifting the gossamer veil., Nature 424 (2003) 625. doi:10.1038/424625a.
[33] T. Xiang, H. G. Luo, D. H. Lu, K. M. Shen, Z. X. Shen, Intrinsic electron and hole bands in electron-doped cuprate superconductors, Phys. Rev. B 79 (2009) 014524. doi:10.1103/PhysRevB.79.014524.
URL http://link.aps.org/doi/10.1103/PhysRevB.79.014524
[34] E. Plekhanov, S. Sorella, M. Fabrizio, Increasing d-wave superconductivity by on-site repulsion, Phys. Rev. Lett. 90 (2003) 187004. doi:10.1103/PhysRevLett.90.187004.
URL https://link.aps.org/doi/10.1103/PhysRevLett.90.187004
[35] Y. Wen, Y. Yu, One-band Hubbard model with hopping asymmetry and the effective theory at finite U: Phase diagram and metal-insulator transition, Phys. Rev. B 72 (2005) 045130. doi:10.1103/PhysRevB.72.045130.
URL https://link.aps.org/doi/10.1103/PhysRevB.72.045130
[36] S. Guertler, Q.-H. Wang, F.-C. Zhang, Variational monte carlo studies of gossamer superconductivity, Phys. Rev. B 79 (2009) 144526. doi:10.1103/PhysRevB.79.144526.
URL https://link.aps.org/doi/10.1103/PhysRevB.79.144526
[37] T. Misawa, M. Imada, Origin of high-T_c superconductivity in doped hubbard models and their extensions: Roles of uniform charge fluctuations, Phys. Rev. B 90 (2014) 115137. doi:10.1103/PhysRevB.90.115137.
URL http://link.aps.org/doi/10.1103/PhysRevB.90.115137
[38] W.-C. Lee, Crossover From Strong to Weak Pairing States in t-J-U Model Studied by A Slave Spin Method, arXiv:1605.03969 (2016).
[39] S. Acharya, A. Medhi, N. S. Vidhyadhiraja, A. Taraphder, Feasibility of a metamagnetic transition in correlated systems, Journal of Physics: Condensed Matter 28 (11) (2016) 116001.
URL http://stacks.iop.org/0953-8984/28/i=11/a=116001
[40] J. Y. Gan, F. C. Zhang, Z. B. Su, Theory of gossamer and resonating valence bond superconductivity, Phys. Rev. B 71 (2005) 014508. doi:10.1103/PhysRevB.71.014508.
URL https://link.aps.org/doi/10.1103/PhysRevB.71.014508
[41] F. Yuan, Q. Yuan, C. S. Ting, Gossamer superconductivity and antiferromagnetism in the t-J-U model, Phys. Rev. B 71 (2005) 104505. doi:10.1103/PhysRevB.71.104505.
URL http://link.aps.org/doi/10.1103/PhysRevB.71.104505
[42] M. Abram, J. Kaczmarczyk, J. Jdrak, J. Spałek, d-wave superconductivity and its coexistence with antiferromagnetism in the t–J–U model: Statistically consistent Gutzwiller approach, Phys. Rev. B 88 (2013) 094502. doi:10.1103/PhysRevB.88.094502.
URL http://link.aps.org/doi/10.1103/PhysRevB.88.094502
[43] B. Liu, X. Yan, F. Yuan, Quasiparticle resonance states induced by a nonmagnetic impurity in gossamer superconductors, Solid State Communications 177 (2014) 123. doi:https://doi.org/10.1016/j.ssc.2013.10.016.
URL http://www.sciencedirect.com/science/article/pii/S0038109813004900
[44] L. Fen-Fen, Z. Yong, Y. Feng, X. Lin-Hua, Effects of the next nearest neighbor hopping on superconductivity and antiferromagnetism of gossamer superconductivity, Communications in Theoretical Physics 57 (4) (2012) 727.
URL http://stacks.iop.org/0253-6102/57/i=4/a=29
[45] K.-K. Voo, Order and excitation in partially Gutzwiller projected $t-t'-t''-J-U$ models, Journal of Physics: Condensed

Matter 23 (49) (2011) 495602.
URL http://stacks.iop.org/0953-8984/23/i=49/a=495602
[46] M. Abram, M. Zegrodnik, J. Spałek, Antiferromagnetism, charge density wave, and d-wave superconductivity in the extended t-J-U model: role of intersite Coulomb interaction and a critical overview of renormalized mean field theory, Journal of Physics: Condensed Matter 29 (36) (2017) 365602. doi:10.1088/1361-648x/aa7a21.
URL https://doi.org/10.1088%2F1361-648x%2Faa7a21
[47] M. Zegrodnik, J. Spałek, Universal properties of high-temperature superconductors from real-space pairing: Role of correlated hopping and intersite Coulomb interaction within the $t-J-U$ model, Phys. Rev. B 96 (2017) 054511. doi:10.1103/PhysRevB.96.054511.
URL https://link.aps.org/doi/10.1103/PhysRevB.96.054511
[48] M. Zegrodnik, J. Spałek, Effect of interlayer processes on the superconducting state within the $t-J-U$ model: Full Gutzwiller wave-function solution and relation to experiment, Phys. Rev. B 95 (2017) 024507. doi:10.1103/PhysRevB.95.024507.
URL https://link.aps.org/doi/10.1103/PhysRevB.95.024507
[49] J. Spałek, M. Zegrodnik, J. Kaczmarczyk, Universal properties of high-temperature superconductors from real-space pairing: $t-J-U$ model and its quantitative comparison with experiment, Phys. Rev. B 95 (2017) 024506. doi:10.1103/PhysRevB.95.024506.
URL https://link.aps.org/doi/10.1103/PhysRevB.95.024506
[50] A. Nocera, N. D. Patel, E. Dagotto, G. Alvarez, Signatures of pairing in the magnetic excitation spectrum of strongly correlated two-leg ladders, Phys. Rev. B 96 (2017) 205120. doi:10.1103/PhysRevB.96.205120.
URL https://link.aps.org/doi/10.1103/PhysRevB.96.205120
[51] Y.-H. Liu, Charge transfer model : What is the effect of charge fluctuation in t-J model, National Tsing Hua University (Master thesis) (2016).
URL https://hdl.handle.net/11296/wz6ru7
[52] Bouchaud, J.P., Georges, A., Lhuillier, C., Pair wave functions for strongly correlated fermions and their determinantal representation, J. Phys. France 49 (4) (1988) 553. doi:10.1051/jphys:01988004904055300.
URL https://doi.org/10.1051/jphys:01988004904055300
[53] H. Yokoyama, M. Ogata, Phase Diagram and Pairing Symmetry of the Two-Dimensional t- J Model by a Variation Theory, Journal of the Physical Society of Japan 65 (11) (1996) 3615. arXiv:https://doi.org/10.1143/JPSJ.65.3615, doi:10.1143/JPSJ.65.3615.
URL https://doi.org/10.1143/JPSJ.65.3615
[54] T. Giamarchi, C. Lhuillier, Phase diagrams of the two-dimensional Hubbard and t-J models by a variational Monte Carlo method, Phys. Rev. B 43 (1991) 12943. doi:10.1103/PhysRevB.43.12943.
URL https://link.aps.org/doi/10.1103/PhysRevB.43.12943
[55] C. T. Shih, T. K. Lee, R. Eder, C.-Y. Mou, Y. C. Chen, Enhancement of Pairing Correlation by $t^{'}$ in the Two-Dimensional Extended $t-J$ Model, Phys. Rev. Lett. 92 (2004) 227002. doi:10.1103/PhysRevLett.92.227002.
URL http://link.aps.org/doi/10.1103/PhysRevLett.92.227002
[56] C. T. Shih, Y. C. Chen, C. P. Chou, T. K. Lee, Absence of the coexistence of superconductivity and antiferromagnetism in the hole-doped two-dimensional extended $t-J$ model, Phys. Rev. B 70 (2004) 220502. doi:10.1103/PhysRevB.70.220502.
URL https://link.aps.org/doi/10.1103/PhysRevB.70.220502
[57] M. C. Gutzwiller, Effect of correlation on the ferromagnetism of transition metals, Phys. Rev. Lett. 10 (1963) 159. doi:10.1103/PhysRevLett.10.159.
URL http://link.aps.org/doi/10.1103/PhysRevLett.10.159
[58] R. Jastrow, Many-body problem with strong forces, Phys. Rev. 98 (1955) 1479–1484. doi:10.1103/PhysRev.98.1479.
URL https://link.aps.org/doi/10.1103/PhysRev.98.1479
[59] K. Kobayashi, H. Yokoyama, Coexistence and Mutual Exclusion of Superconductivity and Antiferromagnetism, and Phase Separation in Hubbard Model, Proceedings of the International Conference on Strongly Correlated Electron Systems (2013). arXiv:https://journals.jps.jp/doi/pdf/10.7566/JPSCP.3.015012, doi:10.7566/JPSCP.3.015012.
URL https://journals.jps.jp/doi/abs/10.7566/JPSCP.3.015012
[60] H. Yokoyama, M. Ogata, Y. Tanaka, K. Kobayashi, H. Tsuchiura, Crossover between BCS Superconductor and Doped Mott Insulator of d-Wave Pairing State in Two-Dimensional Hubbard Model, Journal of the Physical Society of Japan 82 (1) (2013) 014707. arXiv:http://dx.doi.org/10.7566/JPSJ.82.014707, doi:10.7566/JPSJ.82.014707.
URL http://dx.doi.org/10.7566/JPSJ.82.014707
[61] H.-K. Wu, T.-K. Lee, Spectral evolution with doping of an antiferromagnetic Mott state, Phys. Rev. B 95 (2017) 035133. doi:10.1103/PhysRevB.95.035133.
URL http://link.aps.org/doi/10.1103/PhysRevB.95.035133
[62] S. Sorella, Wave function optimization in the variational Monte Carlo method, Phys. Rev. B 71 (2005) 241103. doi:10.1103/PhysRevB.71.241103.
URL http://link.aps.org/doi/10.1103/PhysRevB.71.241103
[63] C. Weber, K. Haule, G. Kotliar, Strength of correlations in electron- and hole-doped cuprates, Nature Physics 6 (8) (2010) 574–578. doi:10.1038/nphys1706.
URL http://www.nature.com/nphys/journal/v6/n8/full/nphys1706.html{#}/ref22{%}5Cnhttp://www.nature.com/nphys/journal/v6/n8/pdf/nphys1706.pdf
[64] C. Weber, K. Haule, G. Kotliar, Apical oxygens and correlation strength in electron- and hole-doped copper oxides, Physical Review B - Condensed Matter and Materials Physics 82 (12) (2010) 1–24. arXiv:1005.3100, doi:10.1103/

PhysRevB.82.125107.
[65] P. Cai, W. Ruan, Y. Peng, C. Ye, X. Li, Z. Hao, X. Zhou, D.-H. Lee, Y. Wang, Visualizing the evolution from the mott insulator to a charge-ordered insulator in lightly doped cuprates, Nat Phys 12 (11) (2016) 1047–1051, letter.
URL http://dx.doi.org/10.1038/nphys3840